Proceedings of 13th European Conference on Turbomachinery Fluid dynamics
Paper ID: ETC2019-307 & Thermodynamics ETC13, April 7-12, 2019; Lausanne, Switzerland

A METHOD FOR MATCHING COMPRESSOR STAGE CHARACTERSTICS TO A GIVEN LOAD PROFILE BY OPERATING POINT WEIGHTING

N. Kienzle[1] - M. Wäsker* - F. di Mare** - Björn Bülten* - C. Doetsch**

*Fraunhofer Institute for Environmental, Safety, and Energy Technology UMSICHT, 45046 Oberhausen, Germany, [1]norman.kienzle@umsicht.fraunhofer.de

**Institute of Energy Technology, Chair of Thermal Turbomachines and Aeroengines, Ruhr-Universität Bochum, 44801 Bochum, Germany

ABSTRACT

A method for the design and revamp of turbomachinery components based on a given load profile is developed and introduced. The procedure is verified by optimizing a single stage vaned centrifugal compressor with respect to different load profiles. A robust optimization methodology is used for carrying out fully automated efficiency optimization on the entire operating range. Three operating point weighted optimization functions are introduced and used as the optimization criterion (objective function). The corresponding efficiencies are calculated by full-stage 3D flow simulation and looped in an automated direct (no meta-model) optimization process using the Adaptive Response Surface Method (ARSM). The aim of the methodology is the utilization of the weighting factors to actively control the operating points (pursuant to their application in a late design or as part of a machinery revamp) and to optimize the efficiency correspondingly. In the test case considered in this work, the diffuser vanes of a centrifugal compressor stage are fully automatically optimized for different distributions of the weighting factors. The procedure for calculating an optimized geometry comprises the setup of a robust workflow and the translation of the load profile into an optimization criterion including boundary definitions. In the test case, nine diffuser design parameters are varied and directly optimized using the direct ARSM. The active control of the efficiency-characteristic between the operating points was verified by varying different weighting factor distributions for two versions (shrouded and unshrouded) of a basic impeller. Results prove the capability of this methodology of matching a stage characteristic to a given load profile.

KEYWORDS

optimization method, centrifugal compressor optimization, compressor revamp

 Copyright © by the Authors
Downloaded from www.euroturbo.eu

NOMENCLATURE

Latin Letters

a	efficiency weighting factor
b	work input weighting factor
ea	ellipsis axis
$\dot{m}$	mass flow
$\mathrm{M_{u2}}$	circumferential mach number
$\dot{m}_{\mathrm{red}}$	reduced mass flow $m_{red} = \dot{m} * 1.7117$
y^+	dimensionless wall distance
AR	aspect ratio
N	rotational speed
OF1	optimization function on mid mass flow
OF2	optimization function on high mass flow
OF3	optimization function on low mass flow
P1	spline point 1st position after leading edge
P2	spline point 2nd position after leading edge
P3	spline point 3rd position after leading edge
P4	spline point 4th position after leading edge
P5	spline point 5th position after leading edge
Z	number of diffuser vanes

Greek

$\alpha_{2,\mathrm{ss}}$	diffuser vane inlet angle (until vane suction side)
η	efficiency
$\beta_{2,\mathrm{R}}$	impeller backsweep angle according to the radial direction
ψ_p	pressure coefficient
ϵ	impeller blade tip gap
2δ	opening angle
Φ_t	flow coefficient

Subscript

cum	cumulated
sh	shrouded
ush	unshrouded
x	direction along camber line
y	direction orthogonal to camber line
i	operating point with respect to mass flow
n	maximum operation
p	polytropic
oa	over-all
2M	measurement radius in the vaneless space
8M	diffuser outlet- and measurement radius
2	impeller outlet radius
3	diffuser vane inlet radius
7	diffuser vane outlet radius

INTRODUCTION

It is very likely that compressor operation behaviour changes during life time. Changes of operation requirements e.g. system bottlenecks, different gas pressure necessities, new process technologies or the need for flexibility due to a higher share of volatile energy can be reasons for that. System operators react e.g. by revamping their existing turbomachinery systems. The goal is to achieve a better matching of the turbomachinery characteristics with the new load profile of the machine in order to lower operating costs. Revamps may include the implementation of improved components (e.g. changed blade/vane shape) or a new design of an entire system. Evaluating load profiles helps to specify economical optimization potentials and define technical modification boundaries. The potential is translated to specifications of new stage characteristics and the level of aerodynamic improvement. Engineers use newest R&D methods to get the best design for the given task and project time frame Using automated optimization algorithms in combination with CFD is a novel method of great interest. Achievements in stage design during the last two decades show great potential in applying this method to turbomachinery R&D, even for multi-objective problems.

In a recent study by Wittrock et al. (2018), an optimization for a centrifugal compressor stage was conducted. The authors show a full stage aerodynamic optimization using 71 parameters including two objective functions (defining range optimum and design point optimum) using a meta model-assisted evolutionary algorithm. The best designs show 2-4% increase in efficiency at design point conditions and a 20% broader operation range. Furthermore Hildebrandt and Ceyrowsky (2018) show an analysis of the behaviour of a centrifugal compressor characteristic towards choke by varying 545 impeller geometries and evaluating the results according to their statistical significance. It was demonstrated, that CFD-driven optimization helps to perform multi-objective optimization regarding stage efficiency, impeller work input and even on pressure slope behaviour towards surge.

Weighting factors are a robust method for reducing multi-objective to single-objective optimization problems stated by Collette and Siarry (2003). In addition, these factors can be used as a connecting link to thermodynamic full machine calculation and customer support e.g. operating hours for different operating points can be translated into optimization goals during (re-)design process of a single stage. This was proposed by Zhao et al. (2014), who introduced a time-averaged method to evaluate compressor performance. They concluded that the approach is able to map a compressors real operating situation rigorously and using a load profile as an optimization criterion is viable.

The usage of a weighted optimization function as an optimization criterion has been investigated in various applications. In the work of Sieverding et al. (2004) a fitness function (weighted multi-objective) is used for aerodynamic optimization of a multi-stage axial compressor blading with the quasi 3D solver (MISES). The authors weighted loss coefficients as well as angles in the same fitness function and used it as objective criterion. In order to enable the usage of the fitness function as a single optimization criterion, the different units of the parameters have to be of the same magnitude. Therefore each parameter is divided by a reference value. Those reference values are chosen from experience or existing profiles. The impact on the characteristics by varying the fitness function is not further investigated in the paper while the authors concluded to find it worthwhile to investigate the influence.

In this work, the operating points are weighted in order to get a single point objective function for direct optimization. Direct optimization has the advantage of having a proved result after every iteration, while indirect methods show lacks in accuracy of the proposed designs.

Furthermore, when indirectly optimizing, best efficiency design may lay in the area of unstable operation.

None of the described works in literature studied the impact of changes of the optimization function in order to control stage characteristics by using direct optimization. The aim of this work is to prove the feasibility of using weighted fitness function by quantifying the impact of the weighting factors. The factors are subsequently modified evaluating the changes in the stage characteristics of a chosen test case.

For the optimizations in this work, geometrical parameters of the stator design are varied, which enable an easy installation by changing nothing more than the diffuser disc and the vanes. This has been done in order to enable the possibility of quick and cheap revamping. Namely, spline points (thickness distribution), nose design (shape of ellipsis) and vane number are varied, keeping outlet angle, in-/outlet radius and channel width constant.

TEST CASE

For verification of the method, the single stage, vaned radial compressor "Radiver" is selected as a reference design. The measurements on this test case Radiver were carried out at the Institute of Jet Propulsion and Turbomachinery at RWTH Aachen, Germany. Part of the investigations was funded by the Deutsche Forschungsgemeinschaft (DFG). Measurements on "Radiver" done by Ziegler (2003) were mainly conducted at 80% speed. As a reason of that, investigations of this work are also performed at this speed. The key figures of this stage are listed in table 1, for 100% and 80% speed. The radial diffuser was modelled by a parametrized radial diffuser design tool. The volute was not part of the model.

For the numerical approach, the SST turbulence model was applied. Between the rotating and stationary domain, the mixing plane model with constant total pressure has been used. The mesh is structured using hexahedrons and the non-dimensional wall distance y+ is kept throughout $<$10 inner wall units. For the mesh independence study, 5 meshes of the Radiver impeller and the initial diffuser (element range impeller+diffuser domain from 182303 up to 3068386) were analysed for the reduced mass flow case $m_{red} = 2.00\frac{kg}{s}$. Grid quality was checked by looking at the minimum and maximum face angle, the element volume ratio and the maximum edge length ratio. As a result of this study a mesh of 515130 elements was chosen.

Impeller

The impeller geometry data made available by the RWTH University was implemented into the meshing tool (ANSYS Turbogrid) via cylindrical coordinates. Even though it is not crucial for verifying the method, the "Radiver" configuration was validated by comparing CFD results to test measurements of Ziegler (2003) (impeller inlet (2M) to diffuser outlet (8M), shown in figure 1). This was done in order to be sure to have a representative geometry for the given flow coefficient. In figure 2 CFD and measurements are compared. A comparison of different radial gaps between impeller blade tip and housing was conducted and showed best agreement for ϵ = 0.4 mm (cold tip-gap was given at ϵ = 0.7 mm). The thermal expansion according to the local temperature at entry and exit of the impeller was neglected, since this would have led to a more elaborate integration of the "Radiver" design. In this work, it is not crucial to replicate the geometry in every detail, as the main focus is on the impact of variations to some referential state.

Diffuser

The radial diffuser is point of interest for the optimization. The parametrization of the geometry is shown in figure 1. It is possible to vary the inlet nose of the diffuser by changing the ratio of the ellipsis axis to each other ($\frac{\mathrm{ea_x}}{\mathrm{ea_y}}$). The thickness is distributed by means of a five point Bézier curve ($\mathrm{P_{1x}/P_{1y}}$, $\mathrm{P_{2x}/P_{2y}}$, $\mathrm{P_{3x}/P_{3y}}$, $\mathrm{P_{4x}/P_{4y}}$, $\mathrm{P_{5x}/P_{5y}}$), while the defining points can be moved in two directions: along camber line (x) and orthogonal to it (y). The number of vanes (Z), the inlet- and outlet angle (α_3, α_7) and the defining radii ($\mathrm{r_2}$,$\mathrm{r_3}$,$\mathrm{r_7}$,$\mathrm{r_{8M}}$,) are held constant.

Table 1: Geometrical parameters and investigated operating conditions of radiver test case Ziegler (2003)

Condition	**Design**	**Investigated**	**Unit**
rotational speed N	35000	28160	rpm
circumferential Mach number $\mathrm{M_{u2}}$	1.44	1.15	[-]
flow coefficient Φ_t	0.044	0.055	[-]
impeller outlet radius $\mathrm{r_2}$	135	135	mm
diffuser inlet radius (measuring point) $\mathrm{r_{2M}}$	139	139	mm
diffuser outlet radius (measuring point) $\mathrm{r_{8M}}$	335	335	mm
backsweep $\beta_{2,\mathrm{R}}$	-38	-38	[°]
mass flow range ($\alpha_{2,\mathrm{ss}}$= 16.5°)$\Delta\dot{\mathrm{m}}$	1.68-2.19	1.68-2.19	kg/s

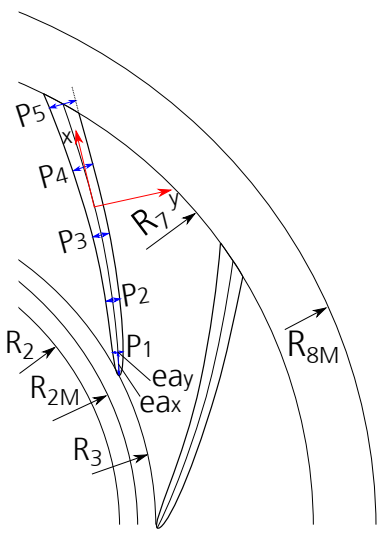

Figure 1: Diffuser parametrization

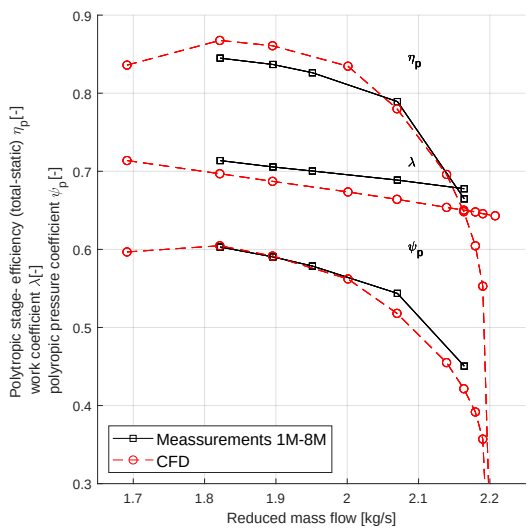

Figure 2: Stage characteristics of "Radiver" centrifugal compressor stage: comparison of CFD results and measurements

METHOD DESCRIPTION

In this section, the procedure of full-range optimization of the stage characteristics is described. Previous internal optimization studies on a transonic compressor did not show satisfactory forecast quality by meta modelling (based on CFD) its behaviour In a direct analysis, a

solver call for each design variation is conducted and therefore the reliability is relatively high. As a reason of that the direct approach is applied.

For the ARSM, an approximation order (linear or polynomial), a DoE scheme and a start range has to be defined. Based on the optimization scheme and the initial geometry a new design set is derived and calculated. The optimal design of the set is then the starting point for the following one. The ARSM is considered to be efficient until up to 20 variables and is a solid procedure for low dimensional single-objective optimization problems. optiSLang software documentation (2017)

The existence of the load profile is required for the method and will not be discussed in this paper. For the verification of the method, fictive load profiles for the centrifugal compressor stage "Radiver" are defined. The procedure is split in two major steps:

- Build up of a robust workflow for the optimization process, including modelling, meshing, preprocessing, obtaining a solution, post processing and the coupling to an effective optimization algorithm
- Translation of load profile into an optimization function (optimization criterion)

Three dimensionless curves are typically used for describing the entire stage characteristics of a compressor. They provide information of specific stage performance for a given flow rate (non-dimensionalized by flow coefficient ϕ), rotational speed (non-dimensionalized by the Mach number M_{u2}) and geometry. Hence, the work input for achieving a certain pressure rise is summarized in these indicators. A schematic presentation of a stage characteristic is given in figure 3.

Only two of the dimensionless curves are required to describe the operational behaviour, because the coefficients are related by $\psi = \eta_p \cdot \lambda$. Therefore, accurate design (control of the slope of the non-dimensional curves) of a stage requires the control of η_p and λ versus ϕ. In this work, weighting factors a_i and b_i are used to weight operating points to each other in order to control the non-dimensional curves of a compressor. The overall 0D operating-point-weighted polytropic stage efficiency referring to the defined range is defined by

$$\eta_{p,oa} = OF_{\eta_p} = \sum_{i=1}^{n} a_i \eta_{p,i}, \tag{1}$$

where the overall operating-point-weighted work input coefficient is defined by

$$\lambda_{oa} = OF_{\lambda} = \sum_{i=1}^{n} b_i \lambda_i, \tag{2}$$

with i characterizing the specific operating point and n the number of operating points per speed line.

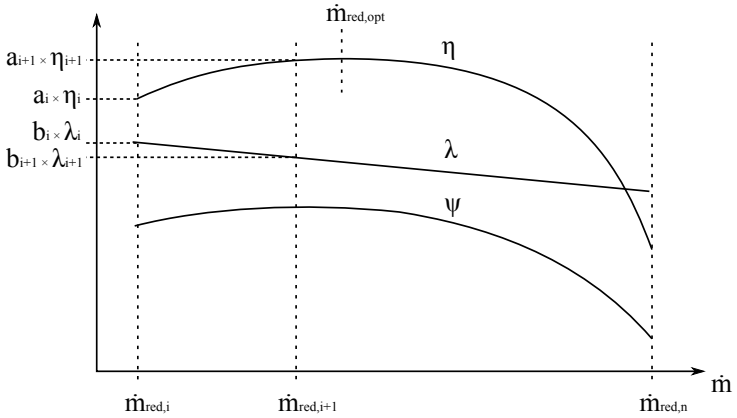

Figure 3: Weighted stage characteristics

Coupling geometry tool, CFD and optimizer (optimization workflow)

In an optimization process the influence of input parameters on one or multiple objective functions is analysed and an optimum input dataset is sought. Therefore in the optimization process, the system itself is a black box returning output values for various input parameters. Different algorithms can be used for optimization, which have various advantages and disadvantages depending on optimization goals and analysed system.

In this work the software *optiSLang V6.2.0* is used. In the software environment a fully-automated system evaluation is implemented returning output values η_p, λ, ψ_p, t_8m, π_8m for the diffuser geometry input values. For each design, various operating points can be calculated and evaluated as signal plots.

The structure of the workflow is linked to a typical CFD analysis: 1. Geometry construction, where a robust modelling enables a wide scope of designs 2. Meshing, which should be evaluated e.g. maximum face angle 3. Calculation setup definition, where special attention should be paid to the start range with the resulting calculation time and the type of optimizing algorithm 4. Calculation, with a system adjusted time-ramp and an interruption control to eliminate unconverged solutions 5. Evaluation by key figures of the system linked to the optimization goal. In this work, only the diffuser geometry is varied. Therefore, only the diffuser geometry construction is parametrized. The diffuser geometry is meshed in *ANSYS Turbogrid V18.0* using pre-defined state files. Calculation and evaluation for various full stage models varying the diffuser geometry is done with the 3D RANS solver *ANSYS CFX V18.0*. Output parameters in the workflow are 0D stage performance values and geometrical values e.g. opening angle, area- and aspect ratio.

Deriving the weighting factors from a given load profile

An example of a load profile is given in figure 4, where the accumulated operating hours per mass flow-interval are shown. The averaged value of the mass flow interval is plotted along the x-axis (e.g. interval i = 1: $m_{red,start} = 1.652$, $m_{red,end} = 1.702$, $m_{red,ave} = 1.68$).

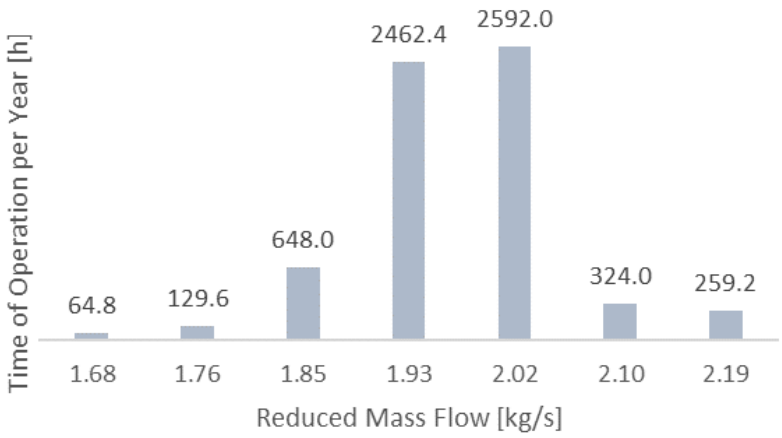

Figure 4: Example of a yearly load profile

The weighting factor for a specific operating point i is then derived by

$$a_i = \frac{\text{Accumulated time of operation for specific operating interval}}{\text{Accumulated time of operation for entire range of stage}} = \frac{t_{\mathrm{i,cum}}}{t_{\mathrm{oa}} = \sum_{\mathrm{i=1}}^{\mathrm{i=7}} t_{\mathrm{i}}} \quad (3)$$

Test plan

The optimization was run six times. Three variations of the objective function (figure 5) combined with two different impeller setups (unshrouded (Radiver) and shrouded (Radiver without tip gap but same outlet width)) were analysed. The flow field of an unshrouded impeller is more complex (higher variation in flow angle because of the tip leakage vortex and recirculation) and might have an impact on the procedure of controlling stage characteristics by radial diffuser optimization.

Parameter ranges

The optimizations were conducted by varying nine diffuser parameters between certain ranges. The inlet and outlet angle of the vanes were kept constant due to an unknown impact of a variation of the outlet angle on the efficiency of the volute (volute not simulated). The inlet angle was kept constant because there is no change in diffuser inlet flow angle expected when changing only the diffuser geometry at the same operating conditions. This assumption was validated by looking at the work coefficient of the impeller shown in figure 6. When comparing the work input for the different optimized designs with the unshrouded impeller, no significant change was observed. The same behaviour was investigated for the shrouded impeller. It must be said that this situation might change when selecting an inlet radius closer to the impeller than the one used in this study ($\frac{R_3}{R_2}$=1.14). Additionally, the diffuser vane number was changed from 13 to 29, where all even numbers are left out in order to prevent onset of forced response (vane number of initial Radiver diffuser is 23). The vane leading edge shape is parametrized by the axis ratio of the inlet ellipsis forming the leading edge. The thickness distribution was varied by the position of different spline points along the camber line of the vane.

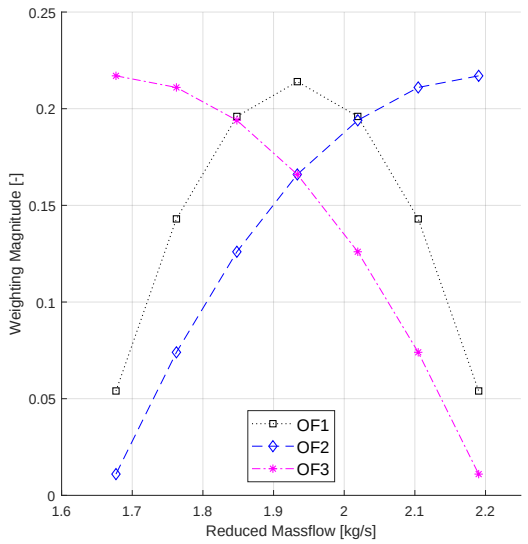

Figure 5: Investigated objective functions

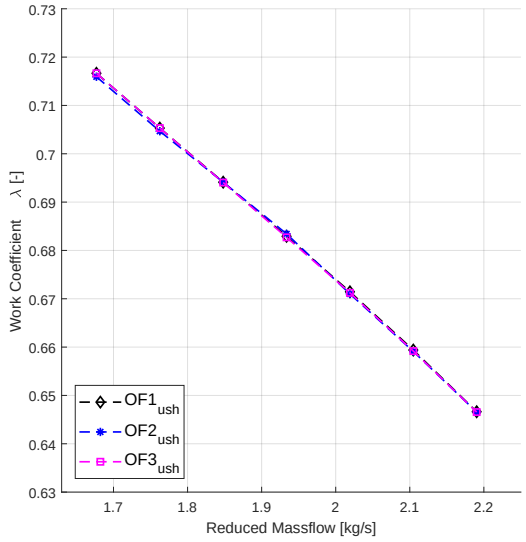

Figure 6: Work input comparison for different optimized diffusers

METHOD VALIDATION - RESULTS

Different optimizations are conducted varying the objective functions (OF1-3) and the impeller geometry (shrouded sh, unshrouded ush).

$$\mathrm{OF}_1 = \eta_{\mathrm{p},1}\cdot 0.054 + \eta_{\mathrm{p},2}\cdot 0.143 + \eta_{\mathrm{p},3}\cdot 0.196 + \eta_{\mathrm{p},4}\cdot 0.214 + \eta_{\mathrm{p},5}\cdot 0.196 + \eta_{\mathrm{p},6}\cdot 0.143 + \eta_{\mathrm{p},7}\cdot 0.054 \quad (4)$$

$$\mathrm{OF}_2 = \eta_{\mathrm{p},1}\cdot 0.011 + \eta_{\mathrm{p},2}\cdot 0.074 + \eta_{\mathrm{p},3}\cdot 0.126 + \eta_{\mathrm{p},4}\cdot 0.166 + \eta_{\mathrm{p},5}\cdot 0.194 + \eta_{\mathrm{p},6}\cdot 0.211 + \eta_{\mathrm{p},7}\cdot 0.217 \quad (5)$$

$$\mathrm{OF}_3 = \eta_{\mathrm{p},1}\cdot 0.217 + \eta_{\mathrm{p},2}\cdot 0.211 + \eta_{\mathrm{p},3}\cdot 0.194 + \eta_{\mathrm{p},4}\cdot 0.166 + \eta_{\mathrm{p},5}\cdot 0.126 + \eta_{\mathrm{p},6}\cdot 0.074 + \eta_{\mathrm{p},7}\cdot 0.011 \quad (6)$$

As an optimization procedure, the adaptive response surface method is applied with linear approximation order and a d-optimal design of experiments method. The 9 parameters conducted then led to a set of 15 designs per iteration. In figure 7 a representative optimization convergence history is shown. In all of the conducted optimizations, a satisfactory convergence was reached after approx. 100-140 design variations.

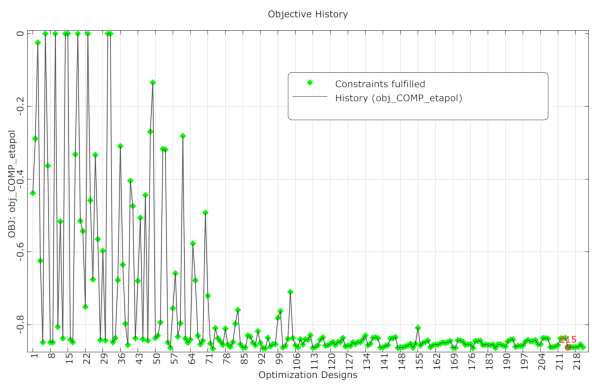

Figure 7: Optimization convergence history for the case of the shrouded impeller with mean flow as the highest weighted optimization criterion ($\mathrm{OF1_{sh}}$)

The analysis of the results is done by looking at the diffuser vane loading (figure 8), the stage efficiency curve (figure 10) and the optimization objectives (table 2). The optimizations were run on a HPC Cluster (Fujitsu Primergy HPC Compute-Node SE-HPC PY RX2530_M2 Rack Server) with 2x Intel XEON E5-2660v4 CPU 2.00 GHz - Turbo 3.2 GHz (14 cores - 28 threads) Processors and 128 GB DDR4. Each of the six calculations were performed on 32 cores, running for approximately eight days. The calculations seemed converged if the standard deviation of the stage polytropic efficiency has dropped below 0.005 (corresponding to an accuracy of $\pm 0.5\%$) for the last 100 iterations at least. If this criterion is not satisfied within 600 iterations, the specific operating point is treated as not converged. It has to be added, that the optimized profiles can have a very thin leading edge and the manufacturing of those profiles can be challenging. Since the demonstration and validation of the method is the main goal of these investigations, manufacturing has not been considered.

The midspan vane loading of the different derived geometries ($\mathrm{GOF1_{sh}}$, $\mathrm{GOF2_{sh}}$, $\mathrm{GOF3_{sh}}$, $\mathrm{GOF1_{ush}}$, $\mathrm{GOF2_{ush}}$, $\mathrm{GOF3_{ush}}$) are shown in figure 8 for the unshrouded impeller and figure 9 for the shrouded impeller. Low mass flow corresponds to a stable point near stall/surge, high mass flow is close to choke and mean mass flow is chosen in the middle of the other operating points. The diffuser geometries (GOF) for the different optimization criteria (OF1-3) are distributed in the rows of the figures. Green highlighted is the specific mass flow for which the design is optimized (GOF2 for high mass flow, GOF1 for mean mass flow, and GOF3 for low mass flow).

Comparing the geometries for the unshrouded impeller for low mass flow operation, $\mathrm{GOF3_{ush}}$ shows a relatively low loading at the leading edge and the first 5% of the stream wise distribution. At 20% stream wise direction, $\mathrm{GOF3_{ush}}$ has already reached the highest pressure on the pressure side. This is due to the high gradient of the pressure distribution in the first 20% of stream wise direction possible, because of the relatively thick leading edge enabling comparable high incidence angles. A smooth vane shape leads to the highest end pressure at the diffuser outlet radius, which also corresponds to the highest total to static stage efficiency. Geometry $\mathrm{GOF2_{ush}}$ has a very high loading at the beginning, leading to a higher pressure on the suction side as on the pressure side at 60% stream wise location. Downstream of this point, no more loading is on the vane and no more pressure rise is generated. These results lead to the highest weighted efficiency of $\mathrm{GOF3_{ush}}$ for low mass flow as can be seen in table 2.

Comparing the loadings at high mass flow (for what $\mathrm{GOF2_{ush}}$ is designed for), profiles $\mathrm{GOF3_{ush}}$ and $\mathrm{GOF1_{ush}}$ show comparable span wise vane loading distributions. These profiles have a lower static pressure at the pressure side of the vane right at the leading edge and this is a cause of flow separation at this point. This flow separation cannot be seen at design $\mathrm{GOF2_{ush}}$, where a smooth vane guidance leads to a high pressure rise in the first 40% of stream wise direction and the loading is almost down to zero at 60%. Flow separation at the end is prevented for the very high opening angle of this profile (14.8°) by increasing the thickness at the trailing edge. Optimized design $\mathrm{GOF2_{ush}}$ has the highest choke-weighted efficiency of the calculated profiles.

The results of the vane loadings of the optimizations with the shrouded impeller are shown in figure 9. Again, for the specific mass flow where the design is optimized for (highlighted in green), this configuration exhibits the highest end pressure in the specific operating point. At mean mass flow the efficiencies of all profiles are almost even at about $\eta_p = 87.5\%$. At high mass flow, the same separation behaviour at the leading edge is observed. Profile $\mathrm{GOF2_{sh}}$ shows the smallest negative slope of the pressure distribution of the suction side leading to the

highest end pressure at this operating point.

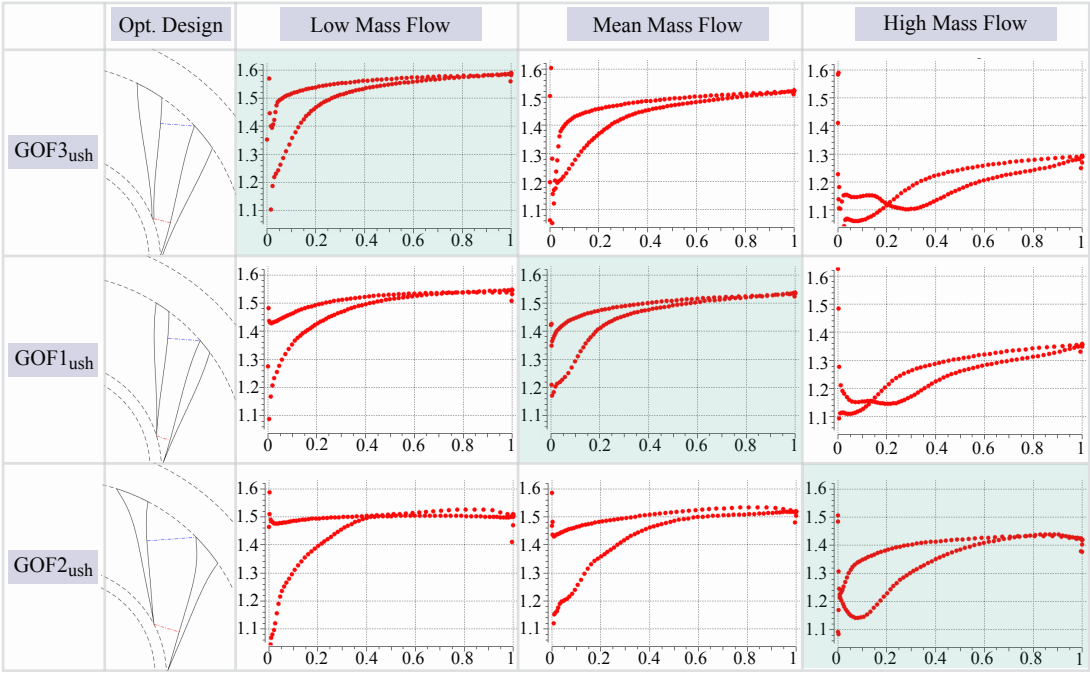

Figure 8: Midspan vane load distributions (pressure (ordinate) along stream wise direction (abscissa)) of the optimized geometries (with unshrouded impeller) with respect to the lowest, mean and highest mass flow in the analysed range

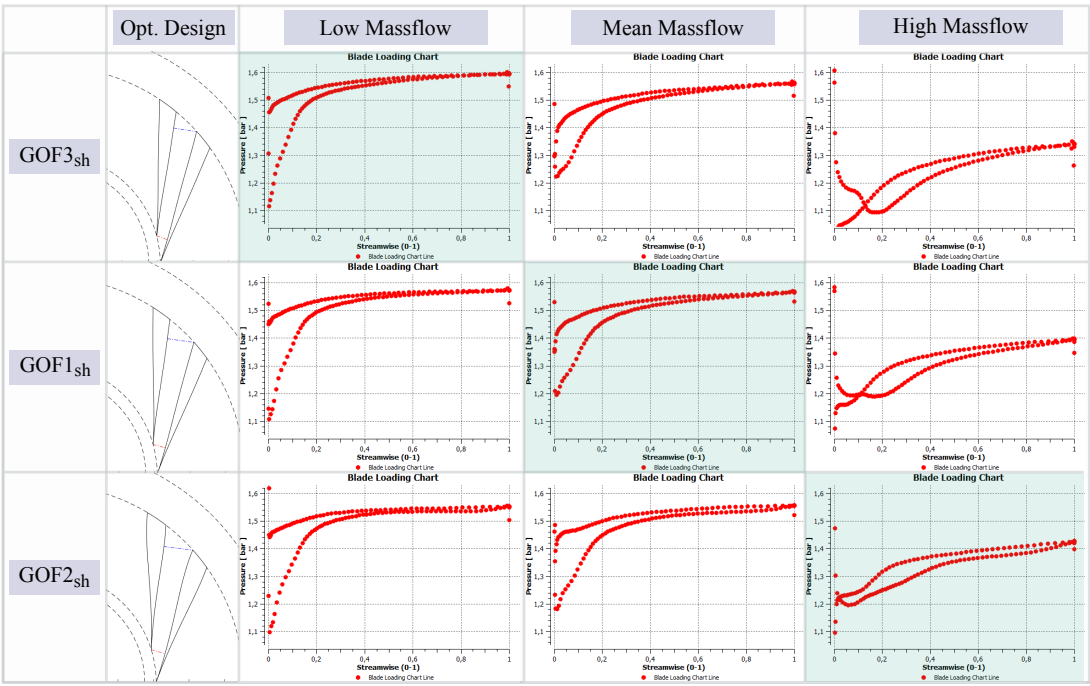

Figure 9: Midspan vane load distributions (pressure (ordinate) along stream wise direction (abscissa)) of the optimized geometries (with shrouded impeller) with respect to the lowest, mean and highest mass flow in the analysed range

In addition to the blade loadings, the resulting polytropic stage efficiency distributions (weighted) for all calculated geometries and mass flows are shown in figure 10. A shift between the curves of the objective functions (See eqs. (4) to (6)) can be qualitatively seen as expected. Furthermore it is shown that profiles for shrouded impellers tend to have higher aspect ratios ($\mathrm{AR}_{\mathrm{sh}} = 0.55 - 0.71$, $\mathrm{AR}_{\mathrm{ush}} = 0.30 - 0.55$) combined with smaller opening angles ($2\delta_{\mathrm{sh}} = 6.3 - 8.1°$, $2\delta_{\mathrm{ush}} = 10.1 - 14.8°$). In general the diffuser vane number is found to have a smaller impact on the optimization chosen in a certain range of vane number. E.g. the five best profiles out of the optimization $\mathrm{OF1}_{\mathrm{ush}}$ have four different vane numbers (21,23,25,27) and all lay in a very similar efficiency range.

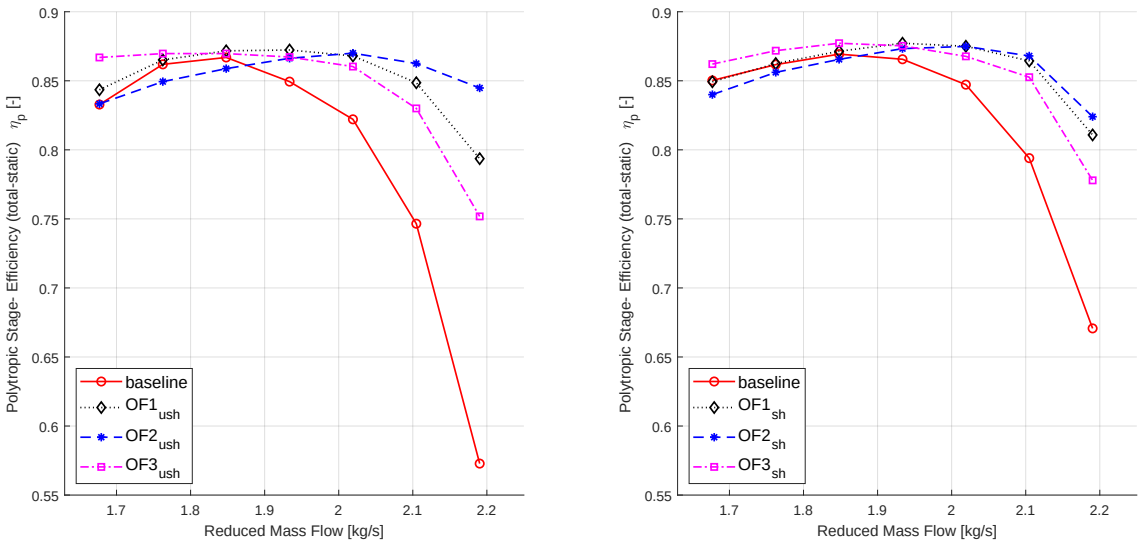

(a) Unshrouded Impeller

(b) Shrouded Impeller

Figure 10: Polytropic stage efficiency characteristics of the differently optimized radial diffuser geometries

Table 2: Weighted polytropic stage efficiency of the optimization test cases (green highlighted are the best diffuser profiles for the given mass flow and impeller type, see figure 8 and figure 9)

Mass flow	Low	Mean	High
$\mathrm{GOF3}_{\mathrm{ush}}$	86.22	85.5	83.25
$\mathrm{GOF1}_{\mathrm{ush}}$	86.04	86.11	84.76
$\mathrm{GOF2}_{\mathrm{ush}}$	85.81	85.97	85.32
$\mathrm{GOF3}_{\mathrm{sh}}$	86.72	86.4	84.62
$\mathrm{GOF1}_{\mathrm{sh}}$	86.4	86.63	85.61
$\mathrm{GOF2}_{\mathrm{sh}}$	85.84	86.39	85.87

CONCLUSIONS

A methodology of matching compressor stage characteristics to a given load profile by diffuser geometry optimization is proposed. Results show the adaptability of the procedure for a centrifugal compressor diffuser. The methodology includes the translation of a load profile into an objective function and the build up of a robust workflow. The object studied has a shrouded and unshrouded impeller setup. The optimized stage efficiency curves show as expected an optimized matching with respect to the load profile of the machine.

ACKNOWLEDGEMENTS

The authors would like to thank Matthias Voss (CADFEM) and Markus Wagner (Dynardo) for their very helpful discussion. This work was partly funded by the Fraunhofer High-Performance Center DYNAFLEX and the German State of North Rhine-Westphalia.

References

Y. Collette and P. Siarry. *Multiobjective optimization: principles and case studies*. Springer-Verlag Berlin Heidelberg, 2003.

A. Hildebrandt and T. Ceyrowsky. 1d and 3d-design strategies for pressure slope optimization of high-flow transonic centrifugal compressor impellers. *Proceedings of ASME Turbo Expo*, 2018.

optiSLang software documentation. *Methods for multi-disciplinary optimization and robustness analysis*. Dynardo GmbH, 2017.

F. Sieverding, B. Ribi, L. Li, M. Casey, and M. Meyer. Design of industrial axial compressor blade sections for optimal range and performance. *Journal of Turbomachinery*, 2004.

D. Wittrock, O. Reutter, E. Nicke, T. Schmidt, and J. Klausmann. Design of a transonic high flow coefficient centrifugal compressor by using advanced design methods. *Proceedings of ASME Turbo Expo*, 2018.

Y. Zhao, J. Xiao, L. Li, Q. Yang, and G. Liu. Performance analysis of centrifugal compressor under multiple working conditions based on time-weighted average. *International Compressor Engineering Conference*, 2014.

K. Ziegler. *Experimentelle Untersuchung der Laufrad Diffusor-Interaktion in einem Radialverdichter variabler Geometrie*. PhD thesis, RWTH Aachen, 2003.

APPENDIX

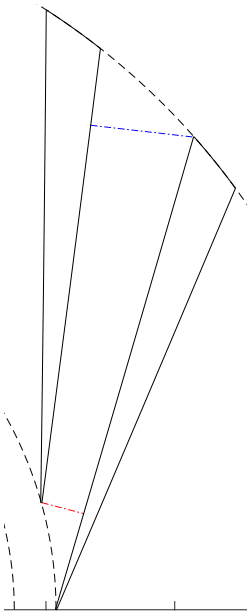

Figure 11: Radiver diffuser baseline design

View publication stats